J Mater Sci: Mater Med (2008) 19:3345–3353
DOI 10.1007/s10856-008-3473-7

Dissolution characteristics of extrusion freeformed hydroxyapatite–tricalcium phosphate scaffolds

H. Y. Yang · I. Thompson · S. F. Yang · X. P. Chi · J. R. G. Evans · R. J. Cook

Received: 15 April 2008 / Accepted: 14 May 2008 / Published online: 11 June 2008

Abstract The dissolution behaviour of calcium phosphate filaments made by extrusion freeforming for hard tissue scaffolds was measured. The solubility of filaments with different HA/β-TCP ratios sintered at temperatures from 1,100 to 1,300°C was measured under simulated physiological conditions (tris buffer solution: tris(hydroxyl) methyl–aminomethane–HCl), pH 7.4, 37°C). Calcium and phosphate concentrations were measured separately by inductively coupled plasma (ICP) atomic emission spectroscopy. Surface morphologies and composition before and after immersion were analyzed by SEM and EDS. The results clearly show that as the β-TCP content increased, the dissolution increased. Higher sintering temperatures, with consequent closure of surface pores, resulted in lower dissolution. Examination of the surface suggested dissolution on preferred sites by pitting.

1 Introduction

Solid freeforming techniques are now available in which multilevel structural hierarchies can be designed on computer and the final component rendered on a building platform using a range of materials and, in some processes, with functional gradients that are themselves also designed on computer [1, 2]. This means that the shape and structure of hard tissue scaffolds that have traditionally relied on a miscellany of natural and synthetic calciferous compounds [3–5] can now be more directly controlled. The method used here is extrusion freeforming, which is similar to fused deposition of ceramics (FDC) [3, 4] and multiphase jet solidification (MJS) [5]. Instead of making use of the solidification of a polymer-ceramic paste to establish the structure, it uses a ceramic paste comprising a polymer vehicle and a volatile solvent and produces solidification by solvent evaporation. Lattice scaffolds are prepared in which each filament welds to the previous layer by growth of the contact area driven by surface energy decrease and resisted by viscosity. In this way, lattice scaffolds with three hierarchical levels of porosity and designed outline shape are established in a computer file, downloaded directly to a building platform and subsequently sintered.

The filament spacing can be varied to give small pores to accommodate cellular activity and mineralization and large pore channels for vascularisation. The overall shape is controlled by using a support structure. All the organic components can be removed by firing at a high temperature to leave a sintered ceramic lattice in which a third level of hierarchical structure, the micro-porosity, is controlled by sintering conditions. We have manufactured HA/TCP ceramic lattices with feature sizes of <100 μm and with three length scales of pore structure at 100–600 μm, 1–100 μm and micro-porosity less than 1 μm [4]. This multilevel structure is believed to play an important role in osteogenesis [6]. It makes sense to apply solid freeforming in this application, not just because of the hierarchical structure it offers but also because the outline shape of patient-specific prostheses can be downloaded from CT datasets, adjusted on computer for

H. Y. Yang · S. F. Yang · X. P. Chi
Department of Materials, Queen Mary, University of London, Mile End Road, London E1 4NS, UK

I. Thompson · R. J. Cook
GKT Dental Institute, Kings College, London SE1 9RT, UK

J. R. G. Evans (✉)
Department of Chemistry, University College London, 20 Gordon Street, London WC1H 0AJ, UK
e-mail: j.r.g.evans@ucl.ac.uk

shrinkage and rendered with multilevel microstructure. It represents rapid prototyping at several scales.

Calcium phosphate based materials, such as hydroxyapatite (HA) and tricalcium phosphate (TCP) are used in implants for orthopaedic and dental applications [7], for bone augmentation, plastic reconstruction, drug delivery systems [8], and bone tissue engineering [9] in the form of blocks, discs, granules or porous scaffolds. Bonelike, apatite hard tissue develops on the surfaces of calcium phosphate based implants which bond to natural bone [10, 11]. Ceramic resorption can occur over a period of months and new bone replaces the artefact [12]. The stages and rates of resorption in a living organism cannot be predicted from conventional laboratory experiments but there is a need for simple comparative tests that can be used to help with compositional and processing decisions.

Many factors affect the solubility of calcium phosphate based materials including the method of preparation, phase content, density, the extent of ionic substitutions into the apatite lattice and microstructure. Their dissolution behaviour varies widely [13]. It is well known that the solubility follows the ranking α-TCP > β-TCP > HA [14, 15]. To modify the dissolution of synthetic HA-based materials, soluble components such as tricalcium phosphate (TCP) are often introduced. Ionic substitution, such as carbonate, disrupts the lattice structure and modifies the dissolution properties [16, 17]. A high level of micro-porosity can also be used to provide more surface area for ion exchange [18].

Simulated body fluids (SBF) and tris–HCl buffer solutions are often used as the immersion environment to assess the in vitro dissolution behaviour of calcium phosphates [6–19]. In SBF, the dissolution processes are often accompanied by precipitation because of the high Ca and phosphate ion concentration in solution. In this study, which is aimed at finding a filament composition that will avoid toxic levels of ion leaching but allow sufficient exchange for bone remodelling, the focus is on the dissolution stage so the tris-buffer system was used.

In order to assess the effects of filament composition and structure on dissolution, stoichiometric HA and β-TCP, meeting ASTM F1185-03 and F1088-04a specifications for clinical applications were used in different ratios as starting materials for filament extrusion. Dissolution was interpreted in terms of phase composition and microstructure after sintering.

2 Experimental details

2.1 Extrusion freeforming of ceramic lattices

The hydroxyapatite ($Ca_{10}(PO_4)_6(OH)_2$, grade P221 S, Plasma Biotal Ltd. UK) and β-tricalcium phosphate ($Ca_3(PO_4)_2$, grade P228 S, Plasma Biotal Ltd. UK) powders were prepared by the manufacturer by calcining at 900°C and milling in water for 96 h. These are better than 95% phase pure as deduced from manufacturer's XRD data, confirmed in our laboratory. Powder blends with different HA/TCP ratios were prepared. The solvent was propan-2-ol (GPR, VWR, UK). Dispersion was carried out with an ultrasonic probe (IKA U200S, IKA Labortechnik SATAUFEN, Germany). Poly(vinyl butyral) (PVB), grade BN18 (Wacker Chemicals, UK) was used as the binder with additions of a grade of poly(ethylene glycol) (PEG) which is liquid at ambient temperature, (M.wt = 600, VWR, UK).

The paste compositions were chosen to give 60 vol.% ceramic based on the dried suspension to prevent the embrittlement of filaments that is found at higher powder loadings. The PVB and PEG600 were fully dissolved in part of the propan-2-ol. Independently, the powder mixture was dispersed by ultrasonic probe in the remaining propan-2-ol for 1 ks. The ceramic suspension was then mixed with the polymer solution and milled on a roller table with zirconia media for 43 ks (12 h). Partial drying with intermittent stirring gave a solvent level suitable for extrusion and the solvent amount remaining at that point was measured by drying a sample to constant mass at 60°C.

The extrusion system consisted of twin micro-extruder screw lines driven by independently controlled micro-stepper motors (50,000 steps/rev) supplied by ACP&D Ltd., Ashton-under-Lyne, UK, with a 64-1 reduction box driving 1 mm pitch ball screws (Automotion Ltd., Oldham, UK). The drives are monitored by load cells (Flintec Ltd., Redditch, UK) that also act as overpressure alarms. The three-axis table (Parker Hannifin, Dorset UK, supplied through Micrometrics, Braintree, UK) is driven by 6k4 motion controller and operated by Labview. The computer control system provides an optional direct and variable ratio drive between table and extruder. The ratio of the speed of extrusion and the x–y motion is calculated by the square of the ratios of the diameters of the extruder barrels and nozzle.

The pastes were loaded into a syringe (HGB81320 1 ml, Hamilton GB, Ltd., Carnforth, UK) fitted with extrusion dies built from sapphire water-jet cutting nozzles of 80, 100, 150 or 300 μm diameter (Types 1708, 1715, 1730, Quick-OHM Kupper & Co. GmbH, Wuppertal, Germany). After drying, the extruded lattices were heated at 5°C/min to 1,100, 1,150, 1,200, 1,250 and 1,300°C separately with a 5 h dwell before furnace cooling to room temperature. Lattices were observed by optical microscopy (Model BX60, Olympus, Japan and by Scanning Electron Microscopy (JSM 6300F, JEOL, Tokyo, Japan). Ceramic plates were also made under the same conditions for XRD analysis (Model D5000, Siemens, Karlsruhe, Germany, using Cu$K\alpha$ radiation). The step size was 0.02 of 2θ with a count time of 2.5 s. Phases were identified using the International Centre for Diffraction Data

powder diffraction files (No. 9-432 for HAP, No. 9-169 for β-TCP, and No. 9-348 for α-TCP). Peaks (2 1 0) for HA and (0 2 10) for β-TCP were used to calculate the ratios of intensities. The surface area of the 100HA filaments were measured by BET (Quantachrome Autosorb 6) using the multipoint method after 24 h preheating at 180°C.

2.2 Dissolution experiments

0.3 g sintered filaments extruded with the 300 μm die were immersed in 200 ml aqueous 0.03 M tris-buffer solution (tris(hydroxyl)methyl–aminomethane–HCl, ex Sigma) at pH 7.3 and at 37°C to investigate the effects of HA/TCP ratio and sintering temperature on dissolution. The calcium and phosphate ion concentrations in the buffer solution for each sample were measured after 2.4 Ms (4 weeks) and 7.8 Ms (3 months) using a inductively coupled plasma (ICP) atomic emission spectroscopy (Perkin Elmer, Optima ICP-OES). Surface morphologies and composition before and after immersion were analyzed by SEM (JSM 6300F, JEOL, Tokyo, Japan) and HR-SEM-EDX (JEOL JSM-6320F EDX, Tokyo, Japan).

3 Results

3.1 Characterisation of sintered filaments

Figure 1a shows the cross section of a sintered filament. A 0–90° lay-up lattice with 100 μm diameter filaments and 50 μm interstices is shown in Fig. 1b. These demonstrate the ability to vary filament diameter and hence macroscopic surface area, interstices and thus both overall volume fraction and mechanical strength. The method allows both smaller pores for mineralization and larger channels to accommodate vascularisation to be designed, an example of which is shown in Fig. 1c. They show that an organised hierarchical structure can be pre-planned and delivered on an individual basis. The downloading time to render a 10 mm cube from 100 μm diameter filaments is about 2.4 ks (40 min). Structures with excellent uniformity can be obtained by automated motion control applied to extrusion of the compliant ceramic paste [20].

Figure 2 shows the rough surfaces and micro-porous structures of the filaments sintered at different temperatures from 1,100 to 1,300°C, the organic components having being oxidatively removed below 600°C. For 1,100°C, there was open porosity in all compositions. The rounding of particles and early stage neck growth, caused mainly by surface diffusion at this low temperature are much more pronounced in the high TCP samples. The HA microstructure retains some angular particles at this stage. Samples with 50HA/50TCP and 75HA/25TCP showed intermediate structures between the end compositions that are shown in Fig. 2. When sintered at 1,200°C, densification was much more extensive particularly at the higher TCP contents, grain size increased and much of the surface porosity was closed, but for nominally 100HA, discrete particles were still visible and much surface porosity remained. All the samples sintered at 1,300°C had closed

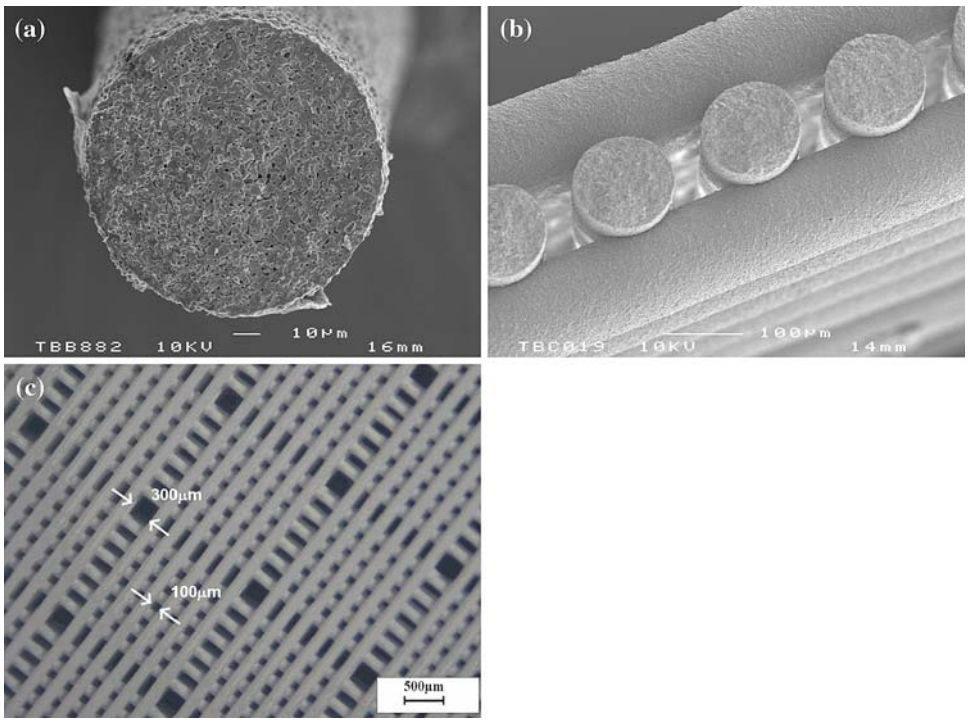

Fig. 1 (**a**) Cross section of filament sintered at 1,200°C, (**b**) section through a lattice of three layers, (**c**) plan view of a lattice with channels designed to encourage vascularisation

surface porosity and significant grain growth. The porosity of the samples extends from nearly 0 to 35% for the different sintering temperatures and compositions [21].

The surface areas of the 100HA samples were measured by BET and the results are shown in Table 1. The filaments sintered at lower temperatures have a higher area surface. The surface areas of the starting powders were 13.1 $m^2\ g^{-1}$ (HA) and 5.3 $m^2\ g^{-1}$ (β-TCP). The results serve to confirm the microstructures of Fig. 2 and, after sintering at 1,250°C, the surface pores are predominantly closed. However, the pores in the bulk may not be fully closed and, since the filaments are broken before insertion in the tube, the N_2 finds some additional inner surface and a higher than expected surface area is recorded. Flexural strength of individual filaments depended on composition and sintering temperature, varying from 30 MPa for 25% HA sintered at 1,100°C to 102 MPa for 75% HA sintered at 1,250°C and will be reported elsewhere in more detail.

Not only do the microstructures and hence strengths change with sintering temperature, but also the ceramic phases may change; for example, HA may decompose to β-TCP and β-TCP can transform to α-TCP above 1,250°C [22]. Since the solubility of HA, β-TCP, α-TCP are different, the dissolution behaviour of the sintered filaments is a complex function of both the phase constitution and microstructure. The composition of the different sintered samples was measured by X-ray diffraction using a calibration method fully described elsewhere [21] and the HA contents in the sintered samples are shown in Table 2. β-TCP was formed after sintering and a small amount of α-TCP was found for 25HA samples and 50HA and 75HA sintered above 1,250°C and for 100HA at 1,300°C. For the samples with small α-TCP peaks, the HA content cannot be exactly defined by the HA/β-TCP calibration method. The significance of the appearance of β-TCP when sintering below 1,200°C in nominally 100HA samples is that there is small amount of calcium deficient HA which transforms above 800°C [23, 24].

Table 1 Specific surface areas of nominally 100HA filaments measured by BET N_2 absorption

Sintering temp. (°C)	Surface area ($m^2\ g^{-1}$)
Unsintered	13.1
1,100	3.9
1,150	4.8
1,200	2.2
1,250	0.5
1,300	1.5

3.2 Dissolution behaviour

Figure 3 shows the results of calcium and phosphate concentration in the tris-buffer solution from filaments after

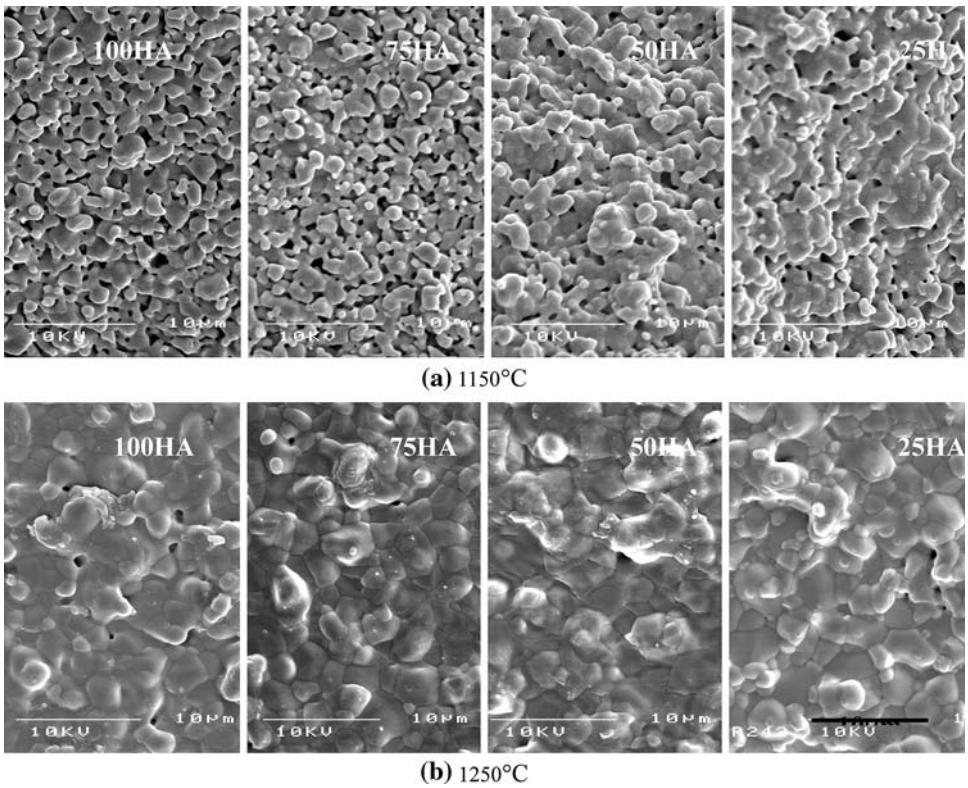

Fig. 2 Surface textures of 300 μm filaments sintered at different temperatures, (**a**) 1,150°C, (**b**) 1,250°C

Table 2 HA weight fraction of the sintered materials[a]

Sample	1,250°C	1,200°C	1,150°C	1,100°C
100HA	0.851	0.832	0.841	0.849
75HA	–	0.651	0.644	0.675
50HA	–	0.36	0.365	0.369
25HA	–	0.141	0.153	0.157

[a] Results are averages of two samples

immersion for 2.4 and 7.8 Ms. The curves demonstrate the effects of immersion time and sintering temperature and allow stoichiometry of dissolution to be assessed. As the sintering temperature increased, the calcium and phosphate ion concentrations resulting from dissolution of the filaments decreased. There is surprisingly little difference in the concentrations of Ca^{2+} between 4 weeks and 3 months and even the phosphate concentration is not greatly changed. Monteiro et al. [16] obtained similar Ca^{2+} ion concentrations (20–45 ppm) from various apatite with initial Ca/P from 1.58–1.68 in SBF after 0.72 Ms. Fazan and Marquis [14] using tris buffer solution, obtained reasonably stable Ca^{2+} concentrations of 42 ppm after 1.2 Ms immersion of plasma sprayed hydroxyapatite coatings but a slight increase with time could still be inferred even after this long immersion. Fulmer et al. [13] show the early stages of dissolution of a commercial carbonated apatite in which the steadily rising Ca^{2+} concentration reaches 7.5 ppm after 0.43 Ms in tris buffer, 37°C. The results in Fig. 3 are therefore in the same range as those obtained by others although clearly phase and chemical purity influences solubility.

To see the effect of dissolution on the surfaces, the morphologies of filaments were investigated by SEM. The changes to surface morphology are not dramatic and on many samples could not easily be detected. Figure 4a shows the surface of 25HA-1,250°C filaments indicating that the dissolution mechanism lead to the formation of cavities on the surface after immersion. The dissolution appears to have taken place on preferred crystallographic planes leaving a series of ridges in the areas that have been attacked. EDX analysis of these areas shows that the Ca/P ratio was 1.56 and for the samples sintered at 1,150°C it was 1.48.

Figure 4b shows that in the 50HA-1,250°C sample, the attack is localised and enlarged surface pores are left. These cavities were formed on a dense surface (Fig. 2b) possibly by enlargement of smaller pre-existing surface pores. More and larger cavities formed at the longer immersion time. The sizes of these cavities are commonly several grain diameters and their angularity is more pronounced than those on the as-sintered surfaces. Figure 4c shows that the resistance to attack seems to increase as the HA content increases and the pores that are present are less deeply pitted but the effect of preferred orientation is apparent.

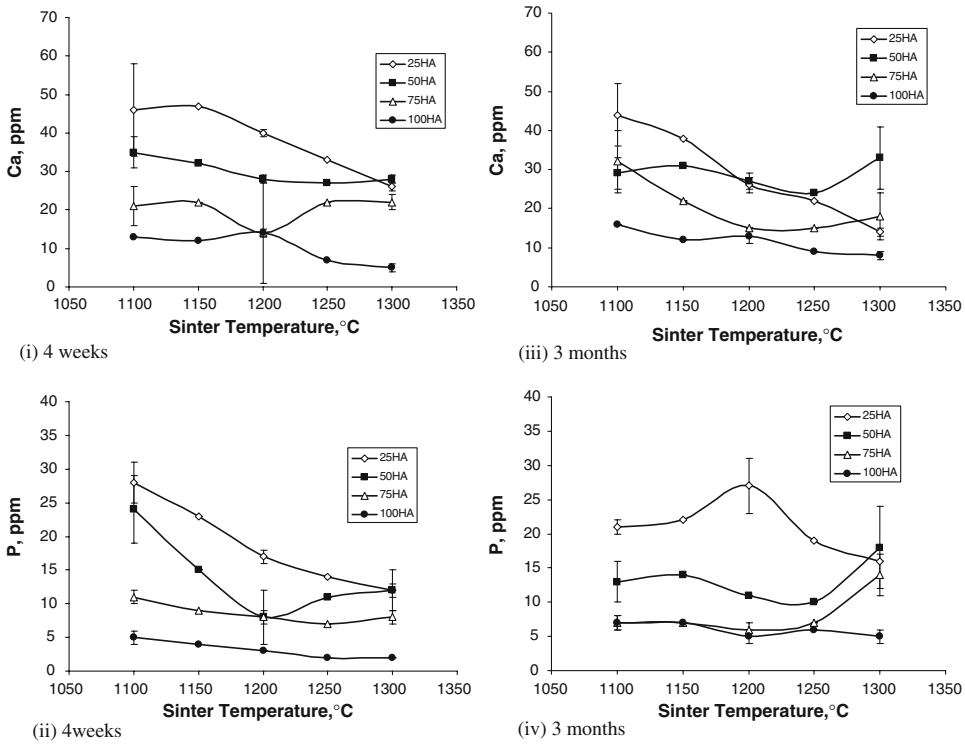

Fig. 3 Calcium (**i**) and (**iii**) and Phosphorus (**ii**) and (**iv**) content in tris-buffer after (**i**) and (**ii**) 4 weeks and (**iii**) and (**iv**) 3 months

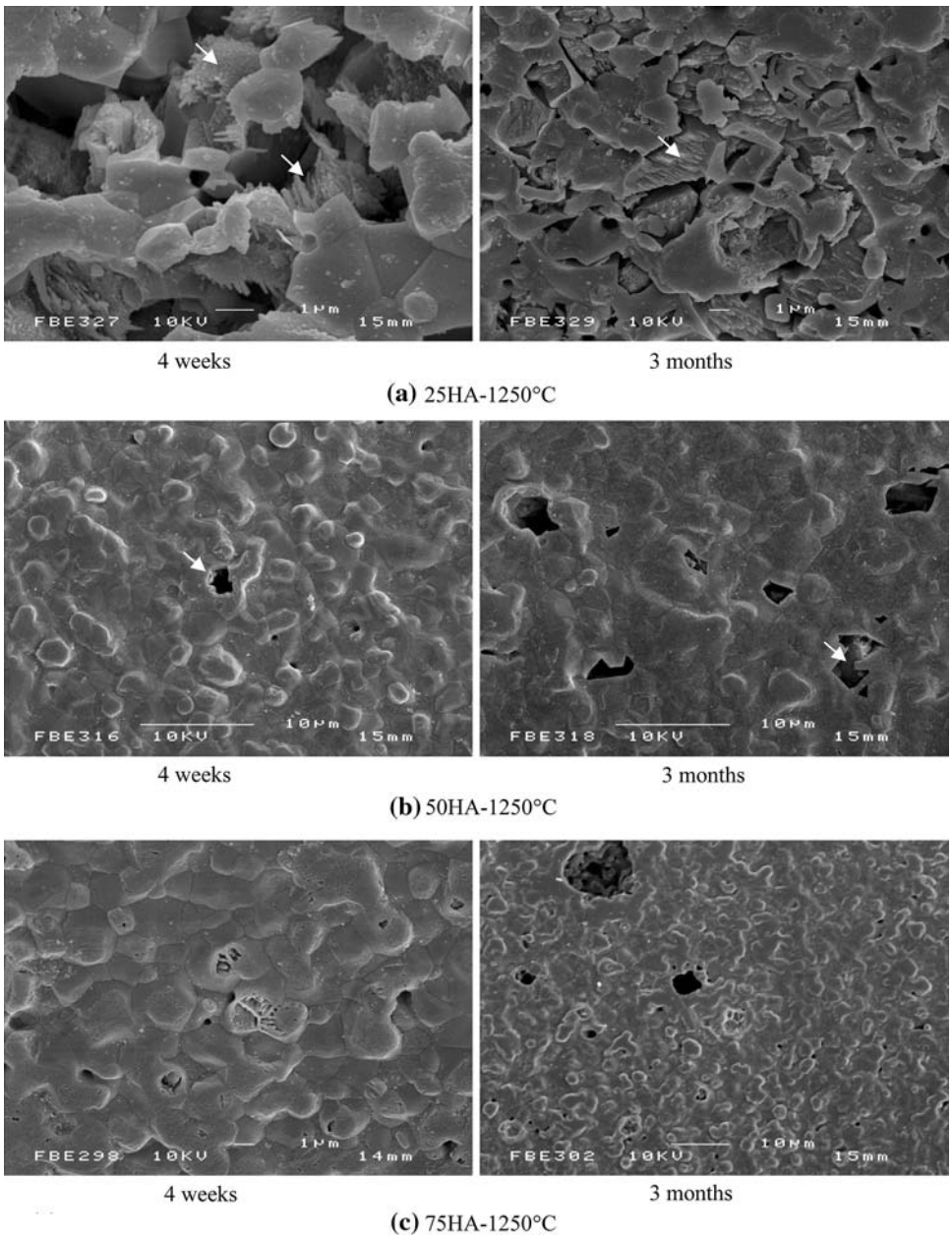

Fig. 4 Surfaces of filaments after immersion in tris-buffer for 4 weeks and 3 months: (**a**) 25HA-1,250°C, (**b**) 50HA-1,250°C (**c**) 75HA-1,250°C

4 Discussion

4.1 Extrusion freeforming of ceramic lattices

Using this extrusion freeforming technique, which provides rapid prototyping at the macroscopic and microscopic scales, a ceramic lattice with defined outline and inner microstructure can be designed in a computer file suitable for development from patient-specific CT data and downloading to a computer peripheral manufacturing centre. A heat treatment stage is needed to remove the organic components and sinter the ceramic powder. Adjustment of the sintering process allows the fine pore structure of the filament to be controlled.

For these two-phase calcium phosphate scaffolds, the composition and microstructure need to be optimised to control dissolution and hence bioactivity. The effects are complicated since the composition and microstructure both depend on the manufacturing stages and the addition of β-TCP not only provides a more soluble composite but also affects the microstructure by enhancing sintering. This may result in increase in resistance to dissolution when the samples are sintered above 1,200°C which tends to produce a predominantly closed surface. These dissolution results

offer a basis for the design of the extrusion freeformed apatite lattices for bone regeneration. Other properties of the lattices, such as strength and biological properties, are needed in order to optimize the product for bone repair and will be discussed elsewhere.

4.2 Dissolution from ceramic filaments

Much work has been done on the dissolution behaviour of calcium phosphate [13, 14, 25, 26], mostly at shorter immersion times (typically less than 2.4 Ms) and most results show that the ion concentrations reach stable values over several days to weeks. This study is extended by comparing the ion concentrations in solution at 2.4 and 7.8 Ms; the results indicating that within experimental error, the majority of samples sintered at a range of different temperatures present no obvious differences in dissolution after 4 weeks and 3 months. There are obvious systematic effects of composition and sintering temperature on dissolution.

HA dissolves very slowly. It may undergo some remodelling by normal biological processes and be partially dissolved but this process may need 2 years or more [27]. This long dissolution time, which may slow down new bone growth, limits the application of single phase HA. These results show that although a porous structure increases the dissolution, increasing the β-TCP content is more effective. Indeed the solubility of the nominally 100HA material is partly due to the appearance, on sintering, of a small amount of β-TCP resulting from calcium deficient HA which cannot be detected by X-ray diffraction in the starting material but can be inferred from the composition after sintering as given in Table 2. Adding TCP is considered to result in faster dissolution in experiments carried out both in vitro, as confirmed here and in vivo and is important for osteoinductivity. Faster dissolution promotes bone-like apatite formation in non-bone tissue [10, 11].

After sintering at above 1,250°C, the filament surfaces were almost fully dense and pitting corrosion rather than uniform dissolution was observed on the surface (Fig. 4a–c). Dissolution appears to begin from favoured sites as previously observed [26] and these may be associated with phase transformations during heating and cooling processes. More dissolution occurs inside the initial pits for two possible reasons. First, the lower localized pH within the pits generated by the dissolved components, which include weak phosphoric acids (e.g. $H_2PO_4^-$, HPO_4^{2-}) [14, 19], can increase the degradation although Wang et al. [26] argue that pH increases in such pits. The angularity of pitting in their surfaces was partly attributed to polishing damage but the surfaces shown here are as-sintered and still show pitting effects. Another reason is that although the surface structure has already been fully sintered, the inside of the filament or cross section still exhibits porosity and hence more local surface area; sub-surface pores may be vulnerable. Porter et al. also confirmed that defects, in particular those involving grain boundaries, were the starting point of dissolution in vivo [28]. Raynaud et al. [25] who also studied pitting effects in Ringer's solution by both surface profilometry and microscopy found that pitting was associated with preferential dissolution of β-TCP grains confirming the view that it is local phase differences rather than geometrical effects that stimulate pitting.

Hydroxyapatite bonds to bone by the formation of a common apatite layer developing on the surface. The precipitation process has been studied both in vivo and in vitro [18, 29, 30]. Apatite layers precipitated on HA in SBF are generally calcium deficient (Ca/P = 1.25–1.66) [31]. Normally, a simulated body fluid (SBF) with ion concentrations nearly equal to those of human blood plasma is used to evaluate the bone-bonding ability of material by examining the ability of apatite to form on its surface in the solution [32]. The solubility product of hydroxypatite in water is very low at 2.34×10^{-59} [33] and the calcium concentration at equilibrium is about 0.44 μM. Fulmer et al. [13] calculated the solubility product in tris buffer pH 7.3, 37°C, for three hydroxyapatite minerals after 0.43 Ms, on the basis that their systems had reached equilibrium. In fact the curves had not reached a plateau which makes the comparison with this work interesting. They found $K_{sp} = 1.2-1.5 \times 10^{-35}$ for their defective apatites and $K_{sp} = 2.9 \times 10^{-42}$ for stoichiometric calcitite. For our materials, sintered at 1,250°C, which have β-TCP contents and minor α-TCP due to the slightly defective HA powder revealed only by XRD on sintered material, the upper and lower limits of Ca^{2+} correspond to 0.40 and 0.13 mM, respectively which give $K_{sp} = 1.1 \times 10^{-32}$ and 3.2×10^{-37} M^9, respectively for tris buffer solution based on stoichiometric HA. The lower value is close to those of Fulmer et al. [13] and the higher value may correspond to the higher concentration that their system may have reached if allowed to continue.

The molar Ca/P ratios deduced from Fig. 3 show that the solution is richer in Ca^{2+} than expected by the stoichiometry of the phosphate from which it was dissolved. Thus when sintering at 1,150°C, for 25HA, molar Ca/P was 1.6 (in solution after 2.4 Ms) instead of 1.54, being the value for that phase composition and for 75HA it was 1.9 (in solution) instead of 1.62. The calcium enrichment of the buffer tended to increase as the sintering temperature rose and as the HA content rose, in line with the stoichiometric ratio so that for nominally 100HA sintered at 1,250°C the ratio in solution was 2.7 after 2.4 Ms. Fazan et al. [14] found a stable ratio developed in their tris buffer solution after a few ks which, when corrected to molar ratio was Ca/P = 2.3, also above that of the undissolved solid.

Tricalcium phosphate–hydroxyapatite mixtures can be dissolved when implanted in the body, followed by precipitation of a hydroxyapatite-like bone mineral [6, 17]. Dissolution and formation of carbonate-containing HA are two of the steps leading to bonelike apatite tissue and bone bonding as observed for HA-coated metal implants and the ectopic osteogenesis with the biphasic ceramics of hydroxyapatite and tricalcium phosphate. But for tissue engineering and some bone defect implantation, faster degradation is needed for the ceramic scaffold to match new bone growth rate. So according to the application, the composition and microstructure and hence the process can be chosen based on these results.

5 Conclusions

Fine lattices with excellent uniformity can be manufactured by extrusion freeforming. The dissolution behaviour of fine filaments made of different HA/TCP ratio powders and sintered at different temperatures were investigated in a tris-buffer medium. The dissolution was continued over 2.4 and 7.8 Ms, extending well beyond other studies. Calcium ion concentrations of 5–55 ppm (0.1–1.4 mM) were in the same range as those measured by others under similar conditions. Results show that the dissolution of these dual phase ceramics decreases as the firing temperature increases and as the tricalcium phosphate content decreases. Values of K_{sp} were in the region 10^{-29}–10^{-35} M^9, comparable to similar work and the Ca/P ratio in solution was consistently higher than that of the solid, rising as the sintering temperature increased.

Acknowledgements The authors are grateful to the Engineering and Physical Sciences Research Council (EPSRC) for supporting this work under Grant Nos. GR/S57068 and EP/E0461193.

References

1. B.Y. Tay, J.R.G. Evans, M.J. Edirisinghe, Solid freeform fabrication of ceramics. Int. Mater. Rev. **48**, 341–370 (2003)
2. S. Yang, K.F. Leong, Z. Du, C.K. Chua, The design of scaffolds for use in tissue engineering Part II: rapid prototyping techniques. Tissue Eng. **8**, 1–12 (2002)
3. I. Grida, J.R.G. Evans, Extrusion freeforming of ceramics through fine nozzles. J. Eur. Ceram. Soc. **23**, 629–635 (2003)
4. F.C. Gomes de Sousa, J.R.G. Evans, Sintered hydroxyapatite latticework for bone substitute. J. Am. Ceram. Soc. **86**, 517–519 (2003)
5. M. Greulich, M. Greul, T. Pintat, Fast functional prototypes via multiphase jet solidification. Rapid Prototyping J. **1**, 20–25 (1995)
6. H. Yuan, K. Kurashina, J.D. de Bruijn, Y.B. Li, K. de Groot, X.D. Zhang, A preliminary study on osteoinduction of two kinds of calcium phosphate ceramics. Biomaterials **20**, 1799–1806 (1999)
7. R. Fujita, A. Yokoyama, T. Kawasaki, T. Kohgo, Bone augmentation osteogenesis using hydroxyapatite and beta-tricalcium phosphate blocks. J. Oral Maxillofac. Surg. **61**, 1045–1053 (2003)
8. B. Peter, D.P. Pioletti, S. Laib, B. Bujoli, P. Pilet, P. Janvier, J. Guicheux, P.-Y. Zambelli, J.-M. Bouler, O. Gauthier, Calcuim phosphate drug delivery system: influence of local zoledronate release on bone implant osteointegration. Bone **36**, 52–60 (2005)
9. B. Leukers, H. Gülkan, S. Irsen, S. Milz, C. Tille, M. Schieker, H. Seitz, Hydroxyapatite scaffolds for bone tissue engineering made by 3D printing. J. Mater. Sci.: Mater. Med. **16**, 1121–1124 (2005)
10. T. Fujiu, M. Ogino, M. Kariya, T. Ishimura, New explanation of the bonding behavior of fluorine containing bioglass. J. Non-Cryst. Solid **56**, 417–422 (1983)
11. K. Kurashina, H. Kurita, Q. Wu, A. Ohtsuka, H. Kobayashi, Ectopic osteogenesis with biphasic ceramics of hydroxyapatite and tricalcium phosphate in rabbits. Biomaterials **23**, 407–412 (2002)
12. G. Takahiro, K. Tatsuyoshi, I. Takuo, Y. Satoshi, K. Hirotaka, Y. Aiichiro, M. Koichi, Resorption of synthetic porous hydrioxyapatite and replacement by newly formed bone. J. Orthop. Sci. **6**, 444–447 (2004)
13. M.T. Fulmer, I.C. Ison, C.R. Hankermayer, B.R. Constantz, J. Ross, Measurements of the solubilities and dissolution rates of several hydroxyapatite. Biomaterials **23**, 751–755 (2002)
14. F. Fazan, P.M. Marquis, Dissolution behavior of plasma-sprayed hydroxyapatite coatings. J. Mater. Sci.: Mater. Med. **11**, 782–792 (2000)
15. P. Ducheyne, S. Radin, L. King, The effect of calcium phosphate ceramic composition and structure on in vitro behavior: I. Dissolution. J. Biomed. Mater. Res. **27**, 25–34 (1993)
16. M.M. Monteiro, N.C.C. da Rocha, A.M. Rossi, G. de Almeida Soares, Dissolution properties of calcium phosphate granules with different compositions in simulated body fluid. J. Biomed. Mater. Res. **65A**, 299–305 (2003)
17. G. Dalculsi, R.Z. Legeros, E. Nery, K. Lynch, B. Kerebel, Transformation of biphase calcium phosphate ceramics in vico: ultrastructural and physicochemical characterization. J. Biomed. Mater. Res. **23**, 883–894 (1989)
18. J. Weng, Q. Liu, J.G.C. Wolke, X. Zhang, K. de Groot, Formation and characteristics of the apatite layer on plasma-sprayed hydroxyapatite coatings in simulated body fluids. Biomaterials **18**, 1027–1035 (1997)
19. K. Hyakuna, T. Yamamuro, Y. Kotoura, M. Oka, T. Nakamura, T. Kitsugi, T. Kokubo, H. Kushitanim, Surface reactions of calcium phosphate ceramics to various solutions. J. Biomed. Mater. Res. **24**, 471–488 (1990)
20. H. Yang, S. Yang, X.P. Chi, J.R.G. Evans, Fine ceramic lattices prepared by extrusion freeforming. J. Biomed. Mater. Res. Part B: Appl. Biomater. **79B**, 116–121 (2006)
21. H. Yang, S. Yang, X.P. Chi, J.R.G. Evans, I. Thompson, R.J. Cook, P. Robinson, Sintering behaviour of calcium phosphate filament for use as hard tissue scaffold. J. Eur. Ceram. Soc. **28**, 159–167 (2008)
22. W. Suchanek, M. Yoshimura, Processing and properties of hydroxyapatite-based biomaterials for use as hard tissue replacement inmplants. J. Mater. Res. **13**, 94–117 (1998)
23. H. Monma, S. Ueno, T. Kanazawa, Properties of hydroxyapatite prepared by the hydrolysis of tricalcium phosphate. J. Chem. Technol. Biotechnol. **31**, 15–24 (1981)
24. A. Mortier, J. Lemaitre, P.G. Rouxhet, Temperature-programmed characterization of synthetic calcium-deficient phosphate apatites. Thermochim. Acta. **143**, 265–282 (1989)
25. S. Raynaud, E. Champion, J.P. Lafon, D. Bernache-Assollant, Calcium phosphate apatites with variable Ca/P atomic ratio III Mechanical properties and degradation in solution of hot pressed ceramics. Biomaterials **23**, 1081–1089 (2002)

26. H. Wang, J.K. Lee, A. Moursi, J.J. Lannutti, Ca/P ratio effects on the degradation of hydroxyapatite in vitro. J. Biomed. Mater. Res. **67A**, 599–608 (2003)
27. W.D. Hollander, P. Patka, C.P.A.T. Klein, G.A.K. Heidendal, Macroporous calcium phosphate ceramics for bone substitution: a tracer study on bidegradation with ^{45}Ca tracer. Biomaterials **12**, 569–573 (1991)
28. A.E. Porter, N. Patel, J.N. Skepper, S.M. Best, W. Bonfield, Comparison of in vivo dissolution processes in hydroxyapatite and silicon-substituted hydroxyapatite bioceramics. Biomaterials **24**, 4609–4620 (2003)
29. F. Lin, C.J. Liao, K.S. Chen, J.S. Sun, C.P. Lin, Petal-like apatite formed on the surface of tricalcium phosphate ceramic after soaking in distilled water. Biomaterials **22**, 2981–2992 (2001)
30. S.R. Radin, P. Ducheyne, The effect of calcium phosphate ceramic composition and structure on in vitro behavior II. Precipitation. J. Biomed. Mater. Res. **27**, 35–45 (1990)
31. N. Kanzaki, K. Onuma, A. Ito, K. Teraoka, T. Tateishi, S. Tsutsumi, Direct growth rate measurement of hydroxyapatite single crystal by moire phase shift interferometry. J. Phys. Chem. B **102**, 6471–6476 (1998)
32. T. Kokubo, H. Takadama, How useful is SBF in predicting in vivo bone activity? Biomaterials **27**, 2907–2915 (2006)
33. H. McDowell, T.M. Gregory, W.E. Brown, Solubility of $Ca_5(PO_4)_3OH$ in the system $Ca(OH)_2$–H_3PO_4–H_2O at 5, 15, 25 and 37°C. J. Res. Natl. Bur. Stds. **81A**, 273–281 (1977)